Research Paper

Volume : 2 | Issue : 9 | September 2013 • ISSN No 2277 - 8179

Synthesis and Characterization of Ni Doped BSCF as a Cathode Material for IT-SOFC

Physics

KEYWORDS : SOFC, nanopowders, cathode, perovskite, area specific resistance.

Suman Kumar Burnwal	Department of Physics, Osmania University, Hyderabad, India
M. Buchi Suresh	Centre for Ceramic Processing, International Advanced Research Centre for Powder Metallurgy and New Materials (ARCI), Balapur, Hyderabad, India
P. Kistaiah	Department of Physics, Osmania University, Hyderabad, India

ABSTRACT

Nanocrystalline powders of Ba0.5Sr0.5CoxFe1-x-yNiyO3-δ (x=0.4; y=0.05. 0.1, 0.15 and 0.2) have been synthesized by sol-gel process. The gel precursors obtained was calcined at various temperatures and the phase evolution was studied by XRD analysis. From the result of X-ray diffraction (XRD) patterns, it is found that a well crystalline cubic perovskite Ba0.5Sr0.5CoxFe1-x-yNiyO3-δ (BSCFNi) was obtained by calcining the precursor at 1000 oC for 4 hrs. Morphological analysis of the samples was done by scanning electron microscope (SEM). TGA results showed the lattice oxygen loss of the product was about ~2 % in its original weight in the temperature range 40-900 oC. In addition, AC impedance data revealed the better electrochemical performance of BSCFNi measured in the frequency range of 0.1 Hz to 1 MHz in relation to their potential use as intermediate temperature (700-800 oC) SOFC cathode. An emphasis is made on the effect of Ni doping on these properties.

1. INTRODUCTION

A key obstacle to reduced temperature operation of SOFC is the poor activity of traditional cathode materials, like LSM, for electrochemical reduction of oxygen in the temperature range of 600-800 °C [1-2]. However, mixed ionic and electronic conductors (MIEC) attract much attention as cathodes due to their unique ability to improve SOFC performance which depends on the oxygen incorporation reaction. MIEC material also plays the role of catalyst in the reduction of oxygen. Mixed ionic-electronic conductivity and a significant open porosity of MIEC material enable oxygen reduction not only on the surface but also in the entire volume of the electrode.

Various transition metals have been investigated on the B-site of perovskite type oxides (ABO_3) as replacements for traditional high temperature cathode materials like LSM. Among the cobalt based materials, BSCF, LSCF, SSC and PBC have been actively reported as candidate materials for IT-SOFC cathodes [3-6]. Perovskite BSCF is a new material with high catalytic activity, which means that oxygen atoms can be reduced as ions as efficient as possible i.e., good oxygen reduction reaction, and it shows an excellent performance as cathode with ceria electrolyte in low and intermediate temperature range. Cobalt and iron based perovskites seems interesting due to their high catalytic activities [7-9].

General trend of oxygen permeation through ceramic membranes was first investigated by Teraoka et al., about two decades ago, based on doped $SrCoO_{3-\delta}$ oxides with the composition of $Ln_{1-x}A_xCo_{1-y}B_yO_{3\pm\delta}$ (Ln–La, Pr, Nd, Sm, Gd; A= Sr, Ca, Ba; B =Mn, Cr, Fe, Co, Ni, Cu) [10-12]. Oxygen diffusion coefficients in the perovskite-type compounds increases in the sequence Cr<Fe<Co, [13, 14] which may imply that in the next of the series Ni has higher diffusion coefficient [15].

In the present work, the emphasis is put on Ni doped BSCF perovskite i.e., $Ba_{0.5}Sr_{0.5}Co_{0.4}Fe_{1-x-y}Ni_yO_{3-\delta}$ for intermediate temperature (700-800 °C) application as cathode of SOFC. BSCFNi perovskite were synthesized to be used as cathode materials for intermediate temperature SOFCs using sol-gel citrate method. The level of Ni substitution for Fe in BSCFNi was varied to study the structural characteristics and AC impedance spectroscopy.

2. EXPERIMENTAL

The samples of $Ba_{0.5}Sr_{0.5}Co_xFe_{1-x-y}Ni_yO_{3-\delta}$ (BSCFNi) powders were prepared using sol-gel citrate method. In this method, stoichiometric amount of nitrate salts of Barium [$Ba(NO_3)_2$]; Strontium [$Sr(NO_3)_2$]; Cobalt [$Co(NO_3)_2$.6H2O]; Iron [$Fe(NO_3)_3$.$9H_2O$]; and Nickel [$Ni(NO_3)_2$.$6H_2O$] were dissolved in double distilled water and stirred it for 6 hours till the complete salts gets dissolved. Citric acid is added to the above solutions in the ratio of 1:1 and stirred for 3 hours till homogeneous solutions are obtained. The pH of the above solution is adjusted to 7 by adding ammonia solution and heated 8 hours at 85 °C until the sol change into gel. The gel formed is heated at 120 °C for 14 hrs, to result in the formation of the black precursor powder of BSCFNi. To increase the homogeneity of the powder, it was subjected to calcinations at 1000°C for 4 hrs, and followed by grinding in an agate mortar. Green pellets of BSCFNi, having a diameter of 13 mm and thickness of ~2 mm, were prepared by pressing the powder uniaxially at a pressure of 10 N/m^2.

X-ray diffraction (Philips X-PERT PRO with Cu-Kα radiation) analysis was carried out on the product obtained for phase purity and structural confirmation. Morphology of the pellet sintered at 1000°C was observed with a scanning electron microscope. The change in weight loss of BSCFNi sample was measured by thermogravimetric analysis (STA449, Netzsch, Germany) in the temperature range of 30-900°C in nitrogen atmosphere.

The electrochemical behaviour of the BSCFNi for varying Ni content was evaluated with electrochemical impedance spectroscopy (EIS). Impedance spectra were measured in the frequency range of 0.1 Hz to 1 MHz and at signal amplitude of 10 mV at 50°C temperature intervals from 300°C to 800°C under an open circuit state for a symmetrical cell with Gadolinium doped Ceria (GDC, purchased from Cottor International, Mumbai, India) electrolytes.

3. RESULTS and DISCUSSION

3.1. X-ray Diffraction Studies

The XRD patterns of the powders of $Ba_{0.5}Sr_{0.5}Co_xFe_{1-x-y}Ni_yO_{3-\delta}$ (x=0.4; $0.05 \le y \le 0.2$) calcined at 1000°C for different concentrations of Ni as dopant are shown in fig 1. It has been reported that the synthesis of the sample through citric route forms undesired secondary phases of Barium and Strontium due to the poor distribution of the alkaline-earth metal (for example, Sr^{2+}) in the solution caused by the relatively weak chelation between Sr^{2+} and carboxylate ligands [16-18]. However, these undesired secondary phases can be removed by calcining at 1000°C. Thus, the synthesized powders were calcined at 1000°C to increase the homogeneity of the powder.

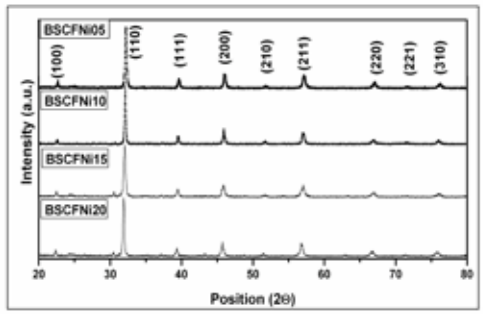

Fig.1.The XRD patterns of the $Ba_{0.5}Sr_{0.5}Co_xFe_{1-x-y}Ni_yO_{3-\delta}$ (x=0.4; 0.05 ≤ y ≤ 0.2) calcined at 1000°C for 4 hrs

The peaks of the XRD patterns of $Ba_{0.5}Sr_{0.5}Co_xFe_{1-x-y}Ni_yO_{3-\delta}$ (x=0.4; 0.05 ≤ y ≤ 0.2) are indexed on the basis of a cubic perovskite phase with the space group Pm3m (221) [19]. The lattice constants for the individual compositions were determined by least square programme, using the XRD pattern.

The crystallite size of the calcined powder is calculated using the Debye-Scherrer equation, Dx = 0.93λ/βcosθ, where λ=1.54178 A° is the wavelength of the X-rays, θ is the diffraction angle and β is full width half maxima (FWHM) [20]. The average crystallite size of the sample powders obtained from the Scherrer formula is 50 nm. Table-1 list the lattice parameters, X-ray densities, relative densities and porosity of $Ba_{0.5}Sr_{0.5}Co_xFe_{1-x-y}Ni_yO_{3-}\delta$ (x=0.4; 0.05 ≤ y ≤ 0.2) samples. The percentage porosity of the samples were measured using the equation, % Porosity = $[(\rho_x - \rho_{exp})/\rho_x] * 100$, where ρx is the X-ray density and ρ_{exp} is the bulk density of the sample. It is observed from the table-1, that the lattice parameter 'a' and porosity increases with increase in Ni content which is also an evident from the XRD result shown in fig.1, as the peaks of BSCFNi shifts towards lower degree as a function of 'y' value showing lattice expansion.

Table-1: Room temperature XRD data for $Ba_{0.5}Sr_{0.5}Co_xFe_{1-x-y}Ni_yO_{3-\delta}$ (x=0.4; 0.05 ≤ y ≤ 0.2)

Sample	Ni conc.	Lattice constant (°A)	X-ray density (gm/ cm^3)	% Porosity
BSCFNi05	0.05	3.960	5.820	20.58
BSCFNi10	0.1	3.969	5.785	21.15
BSCFNi15	0.15	3.976	5.758	23.65
BSCFNi20	0.2	3.981	5.740	25.71

The increase in the lattice parameter or expansion of the lattice could be explained as follows: the ionic radii of Nin+ are smaller than those of Fen+ with the same valence (r_{Fe3}+=0.79 Å, r_{Ni3}+=0.74 Å, r_{Fe4+}=0.73 Å, r_{Ni4+}=0.62 Å), so the equivalent substitution of Ni for Fe cannot bring about this variation of lattice parameter 'a'. This implies that Ni ions in BSCFNi materials may take the Ni^{3+} state rather than the Ni4+ state, and the Ni^{3+} ions replace parts of Fe^{4+} ions leading to expansion of the lattice. The incorporation of Ni leads to the decrease of average valence of B-site elements in the perovskite; this may be compensated by the formation of oxygen vacancies and thereby maintaining the electrical neutrality condition. The formation of oxygen vacancies or oxygen loss in the sample can be confirmed by TGA.

3.2. SEM Analysis

Figure 2(a-d) shows the SEM micrograph taken on the pellets of $Ba_{0.5}Sr_{0.5}Co_xFe_{1-x-y}Ni_y$ sintered at 1000 °C. The micrograph suggests that the material comprises of polycrystalline microstructure and the grains are homogeneously distributed throughout the fracture surface. The presence of highly porous particles with a nano-metric grain size, varying between 1 to 2 µm, is observed in the morphology obtained in this work, which resembled the typical cathode structure for SOFC.

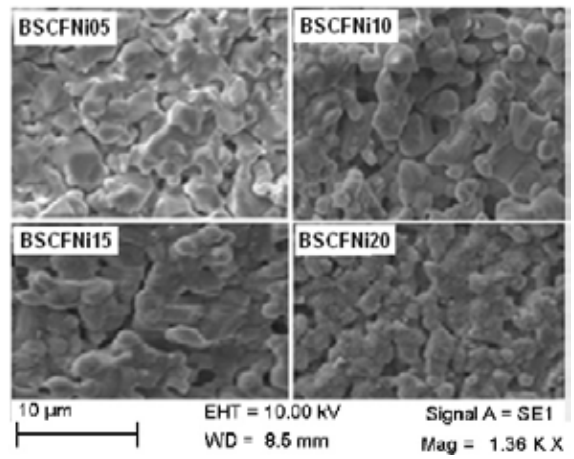

Fig.2. SEM micrograph of $Ba_{0.5}Sr_{0.5}Co_xFe_{1-x-y}Ni_yO_{3-\delta}$ (x=0.4; 0.05 ≤ y ≤ 0.2) pellets sintered at 1000°C

3.3. Thermogravimetric Analysis

TGA results shown in fig. 3 gives the lattice oxygen loss of the product, which is obtained about ~2.107% for BSCFNi10 and ~2.263% for BSCFNi15 in its original weight in the temperature range of 40-900°C. This loss may have come on account of maintaining the overall electrical neutrality of the sample, as the Ni doping decreases the average valence of B-site elements in the perovskite. It can also be observed from the fig. 3 that there is know further oxygen loss takes place after 900°C. The TGA result obtained for $Ba_{0.5}Sr_{0.5}Co_xFe_{1-x-y}Ni_yO_{3-\delta}$ showed about ~2% lattice oxygen loss of the product in its original weight in the temperature range of 40-900 °C [21]. The observed weight loss during heating is due to the loss of oxygen from the lattice, which results in the formation of oxygen vacancies and the valence change of the metal ion [22].

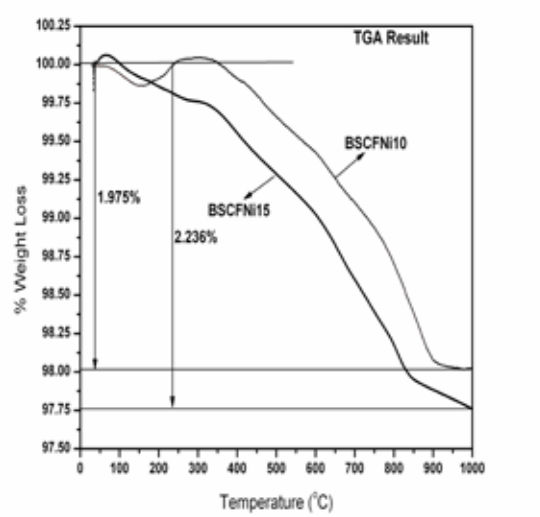

Fig.3. TGA graph showing weight % loss for BSCFNi10 and BSCFNi15 samples

3.4. A.C. Impedance Measurement

The impedance spectra, shown in fig. 4 and 5, is measured for a symmetrical cell with Gadolinium doped Ceria (GDC) electrolytes i.e., BSCFNi/GDC/BSCFNi under an open circuit voltage (OCV) in the frequency range of 0.1 Hz to 1 MHz.

Volume : 2 | Issue : 9 | September 2013 • ISSN No 2277 - 8179

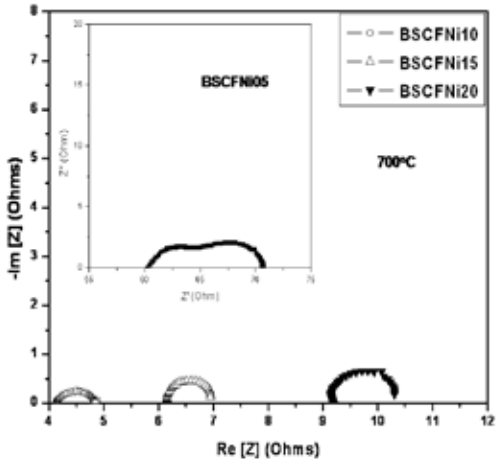

Fig.4. AC Impedance spectra of the $Ba_{0.5}Sr_{0.5}Co_xFe_{1-x-y}Ni_yO_{3-\delta}$ (x=0.4; 0.05 ≤ y ≤ 0.2) at 700 °C

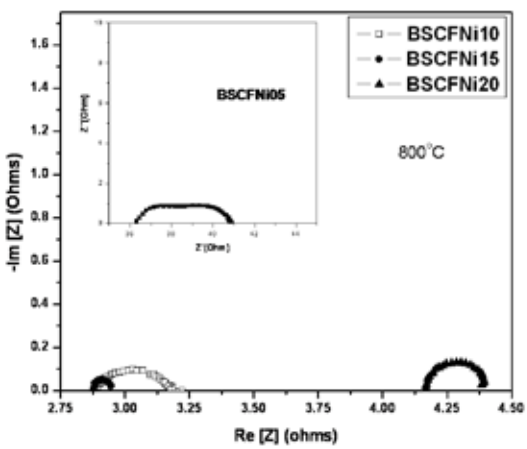

Figure-5: AC Impedance spectra of the $Ba_{0.5}Sr_{0.5}Co_xFe_{1-x-y}Ni_yO_{3-\delta}$ (x=0.4; 0.05 ≤ y ≤ 0.2) at 800 °C

The area specific cathode resistance (ASR) is calculated as a characteristic measure for the MIEC cathode performance. The ASR values of the BSCFNi measured for varying Ni concentration at 700 and 800 °C are shown in table-2. It is observed from the table that the ASR values decreases with increase in Ni concentration, except for y=0.2. In this work, the BSCFNi10 and BSCFNi15 electrode sintered at 1000 °C has the ASR values 0.43 Ω-cm2 and 0.29 Ω-cm2 at 700 °C which is comparable to 0.26 Ω-cm2 obtained for $Ba_{0.5}Sr_{0.5}Co_{0.2}Fe_{0.8}O_{3-\delta}$ and 0.18 Ω-cm2 for $Ba_{0.5}Sr_{0.5}Co0._{15}Fe_{0.8}$ $Zn_{0.0}5O_{3-\delta}$ (BSCZF05) at 700 °C. The ASR values of BSCFNi10 and BSCFNi15 electrode obtained at 800 °C are 0.08 Ω-cm2 & 0.04 Ω-cm2 respectively which is better than the BSCZF05-SDC composite electrode having ASR value of 0.09 Ω-cm2 at 700 °C [23] and is also comparable to the ASR values of $Ba_{0.5}Sr_{0.5}Co_{0.8}Fe_{0.2}O_{3-\delta}$ (0.032 Ω-cm2, sample sintered at 900 °C) obtained at 700 °C [24].

Table-2: ASR values for $Ba_{0.5}Sr_{0.5}Co_xFe_{1-x-y}Ni_yO_{3-\delta}$(x=0.4; 0.05 ≤ y ≤ 0.2) measured at 700 °C and 800 °C.

Sample	Ni conc.	ASR (Ω-cm^2)	
		700 °C	800 °C
BSCFNi05	0.05	6.60	0.72
BSCFNi10	0.10	0.43	0.08
BSCFNi15	0.15	0.29	0.04
BSCFNi20	0.20	0.75	0.14

The ASR values mainly depend on particle size, sintering temperature and microstructure of the sample. The lowest ASR values were obtained for BSCFNi10 and BSCFNi15. The lower values of ASR for BSCFNi cathode is due to cathode microstructure being more porous as shown in table-1, as a result of which gas diffusion phenomenon is enhanced to facilitate better oxygen reduction [25]. The oxygen reduction behaviour could also be explained in terms of the lattice expansion. The lattice expansion of the samples of BSCFNi increases with increase in the nickel concentration which results in the formation of oxygen vacancies as the larger Ni^{3+} (0.74 Å) cation replaces the smaller Fe^{4+} (0.73 Å) cation at the B-site of ABO_3 perovskite structure. The loss of oxygen in the lattice can be seen in TGA result. It is known that the oxygen vacancies on the electrode surface or in the electrode provide the reaction site for the reduction of molecular oxygen and the pass way for the diffusion of reduced oxygen ions [26-28]. Thereby changes the resistance of oxygen adsorption or desorption and the oxygen ions diffusion in the electrode to good extent; higher the oxygen vacancies concentration of a cathode material lower is their ASR. The increase in the ASR for BSCFNi20 (y=0.2) could be due to the Ni dopant concentration exceeding a certain value called percolation limit, at which electronic conduction becomes predominant [29].

4. CONCLUSION

$Ba_{0.5}Sr_{0.5}Co_xFe_{1-x-y}Ni_yO_{3-\delta}$(BSCFNi; x=0.4; 0.05 ≤ y ≤ 0.2) perovskite oxides were prepared using sol-gel citrate method and examined as a new IT-SOFC cathode material. The samples were calcined at 1000°C to remove any secondary phases to yield well crystallized BSCFNi powders. The effect of Nickel doping on the microstructure, oxygen loss and ASR was investigated and it was found that Ni doping concentration of x= 0.1and 0.15 has the lowest area specific resistance measured at 700 and 800°C. Thus the BSCFNi with optimum Nickel doping level can be a good candidate as cathodes for intermediate temperature SOFCs application.

REFERENCE

[1] Yasuda, I., Ogasawara, K., Hishnuma, M., Kawada, D., Dokiya, M. (1996), Solid State ionics, 1197, 86-88. [2] Kostoglodius, G. Ch., Ftikos, Ch.(1999), Solid State ionics, 126, 143. | [3] Liu, Q. L., Khor, K. A., Chan, S. H. (2006), Journal of Power Sources, 161, 123-8. | [4] Tietz, F., Haanappel, V.A.C., Mai, A., Mertens, J., Stover, D. (2006), Journal of Power Sources, 156, 20-2. | [5] Zhang, X., Robertson, M., Yick, S., Deces-Petit, C., Styles, E., Qu, W. (2006), Journal of Power Sources, 160, 1211-6. | [6] Kim, G., Wang, S., Jacobson, A. J., Reimus, L., Brodersen, P., Mims, C. A. (2007), Journal of Material Chemistry 17, 2500-5. | [7] Wei, B., Lu, Z., Huang, X., Miao, J., Sha, X., Xin, X., Su, W. (2006), J. European Ceramic Society, 26, 2827. | [8] Jung, J. I., Misture, S. T., Edwards, D. D. (2009), Journal of Electroceramics, 4. | [9] Yong, Ho. Lim., Jun, Lee., Jong, Seol. Yoon., Chul, Eui. Kim., Hae, Jin. Hwang. (2007), Journal of Power Sources, 171, 79-85. | [10] Teraoka, Y., Zhang, H. M., Furukawa, S., Yamazoe, N. (1985), Chem. Lett., 14, 1743. | [11] Teraoka, Y., Nobunaga, T., Yamazoe, N. (1988), Chem. Lett. 17, 503. | [12] Teraoka, Y., Nobunaga, T., Okamoto, K., Miura, N., Yamazoe, N. (1991), Solid State Ionics, 48, 207. | [13] Van Hassel, B. A., Kawada, T., Sakai, N., Yokokawa, H., Dokiya, M., Bouwmeester, H.J.M. (1993), Solid State Ionics, 66, 295. | [14] Ishigaki, T., Yamauchi, S., Kishio, K., Mizusaki, J., Fueki, K. (1988), J. Solid State Chem., 73, 179. | [15] Kharton, V.V. et al. (2000), Solid State Ionics, 132, 119-130. | [16] Pena-Martinez, J., Marrero-Lopez, D., Ruiz-Morales, J. C., Nunez, P., Sanchez-Bautista, C., Dos Santos-Garcia (2009), International Journal of Hydrogen Energy, 34, 9486-95. | [17] Pena-Martinez, J., Marrero-Lopez, D., Ruiz-Morales, J. C., Buergler, B. E., Nunez, P., Gauckler, L. J. (2006), Solid State Ionics, 177, 2143-7. | [18] Huang, K., Wan, J., Goodenough, J. B. (2001), Journal of Material Science, 36, 1093-8. | [19] Koster, H., Mertins, F. H. B. (2003), Powder Diffraction, 18, 56-59. | [20] Warren, B. E. (1990), X-ray Diffraction, Dover, New York, p. 251. | [21] Subramania, A., Saradha, T., Muzhumathin, S. (2007), Journal of Power Sources, 165, 728-732. | [22] Tai, L.W., Nasrallash, M.M., Anderson, H.U., Sparlin, D.M., Sehlin, S.R. (1995), Solid State Ionics, 76, 259. | [23] Jungdeok Park, Jing Zou, Heechul Yoon, Guntae Kim, Jong Shik Chung (2011), International Journal of Hydrogen Energy, XXX, 1-10. | [24] Chiung-Hsun Chen, Chun-Liang Chang, Bing-Hwai Hwang (2009), Materials Chemistry and Physics, 115, 478-482. | [25] Wei Zhou, Ran Ran, Zongping Shao (2009), Journal of Power Sources, 192, 231-246. | [26] Ishihara, T., Kudo, T., Matsuda, H., Takita, Y. (1995), Journal of Electrochemical Society, 142, 1519. | [27] Kim, S., Wang, S., Chen, X.,Yang, Y.L., Wu, N., Ignatiev, A., Jacobson, A. J., Abeles, B. (2000), Journal of Electrochemical Society, 147, 2398. | [28] Horita, T., Yamaji, K., Sakai, N., Yokokawa, H., Kawada, T., Kato, T. (2000), Solid State Ionics, 127, 55. | | [29] Kharton, V.V., Yaremchenko, A.A., Naumovich, E.N. (1999), Journal | of Solid State Electrochem., 3, 303. | | |